onset was 44 years old and the average duration of illness was 8.5 years. Initial symptoms and signs in 7 cases were of bvFTD, which is consistent with reports from western countries [3,10,11]. It has to be noted that cases 2 and 3 were included in two of the previous studies with FUS immunohistochemistry [5,10], and case 9, a case with unusual FUS pathology, has been reported elsewhere [25].

The details of the clinical and pathological features, except for the FUS immunopathology, were reported previously in cases 1–7 and 9 [19,26–33]. In summary, the brain weights ranged from 880 to 1230 g. The distribution of cerebral atrophy varied from case to case, although it was confined to either the frontal or the temporal cortex or both (Table 3). All cases showed severe atrophy of the caudate head. The detailed distribution and severity of degeneration in cases 1–4, 6, 7 and 9 have been described in previous reports [19,25], so we have added the corresponding data for cases 5 and 8 and assembled them into supplementary Fig. 1. Of the newly added cases, case 5 was fully compatible with BIBD and case 8 appeared to be aFTLD-U, although the number of NII was modest. Various numbers of round or oval-shaped NCIs were found with HE (Fig. 1A), KB and Bodian's silver stainings in the affected CNS regions in cases 1 through 7. The broad distribution of NCIs in the 4 BIBD cases, cases 1 through 4, and 2 NIFID cases was reported previously [5,10,19,31]. In case 5, NCIs were present similarly to other BIBD cases in the frontal and temporal cortices, hippocampus, amygdala, basal ganglia and brain stem nuclei such as the pontine nucleus. In an NIFID case, case 6, a few NCIs in the hippocampus contained eosinophilic cores (Fig. 1B) [11,15,17,19] and, in the other NIFID case, case 7, some NCIs had faintly stained compartments outlined with relatively intense staining with HE and KB (Fig. 1C) [15]. In cases 8 and 9, no NCIs were discerned with HE and KB staining.

Ubiquitin immunohistochemistry revealed a small number of NCIs in cases 5, 6, 8 and 9 but not in other cases. In case 8, only occasional ubiquitin-positive vermiform NIIs were seen and limited to the hippocampal dentate granular cells. In the two NIFID cases, many NCIs were positive for α-internexin (Fig. 1D). α-Internexin positive NCIs were also present, though rare, in cases 1 and 4. In the other cases, no apparent α-internexin positive inclusions were found, but diffuse and intense neuronal cytoplasmic staining was seen frequently in degenerated brain regions. Such intense cytoplasmic staining was often difficult to distinguish from crescent and annular NCIs.

FUS immunohistochemistry showed numerous NCIs and a few DNs in the frontal and temporal cortices in cases 1 through 8. The NCIs bearing eosinophilic core in case 6 were positive for FUS, but the cores themselves were either negative or only weakly positive for FUS (Fig. 1E)

Table 3
Findings of FUS immunohistochemistry using multiple antibodies.

Case #		1	2	3	4	5	6	7	8	9
Epitope	1–50 (Bethyl)	I	I	I	I	N	N	N	I	N
	1–50 (Abcam)	I	I	I	I	U	N	N	I	I
	52–400	I	I	I	I	I	I	I	I	I
	86–213	I	I	I	I	I	I	I	I	I
	250–300	–	I	–	–	–	I	U	–	–
	400–450	U	U	N	N	N	N	N	N	N
	500–526	–	–	N	N	N	N	N	N	–

I: inclusions are stained more readily than the nuclei; N: the nuclei are stained more readily than inclusions; U: the difference between the nuclei and inclusions is unclear; –: no positive staining is obtained.

Fig. 1F illustrates that the NCIs visible on HE-stained sections are variably immunoreactive for FUS. In cases 1 through 7, the size and morphology of NCIs were variable, being annular, crescent, tangle-like, oval or round (Fig. 1G), while, in case 8, small, round NCIs predominated in the cerebral cortex (Fig. 1H). GCIs were found only in cases 1, 6 and 7. Sparse NIIs were seen in the hippocampal CA1, transentorhinal cortex, globus pallidus and putamen in case 7 (Fig. 1I) and in the hippocampal dentate granular cells in case 8 (Fig. 1J). Case 9 was atypical in that DNs predominated over NCIs in the cerebral cortex (Fig. 1K) and that, in addition to FUS accumulation in the brain, TDP-43 positive NCIs were present in the brain stem and the spinal cord. TDP-43 positive inclusions were not seen in the other 8 cases. The details of case 9 were reported elsewhere [25,30]. The FUS pathology of this case did not correspond to any known subtype. In summary, FTLD-FUS subtypes in this archive are as follows: 5 BIBD, 2 NIFID, 1 aFTLD-U and 1 unclassifiable.

Because of the inconstant staining intensity of FUS immunohistochemistry among cases, we applied multiple antibodies that were raised against various portions of the FUS molecule to the neocortex and hippocampus sections of all cases. The results of FUS immunostaining with these antibodies were variable, depending on the localization of antigen epitopes, and could be divided into two patterns: type I in which NCIs and DNs were more intensely or readily stained than the neuronal nuclei, and type N in which nuclei were stained better than the inclusions (Figs. 2 and 3). If the difference in staining intensity was not easily evident, the patterns were determined by staining the sections at different concentrations of the antibody. In type I, NCIs were stained positively at a lower concentration than

Table 2
Clinical and pathological features.

Case no./sex	Age at onset, year	Disease duration, year	Initial symptoms	Prominent features	Cerebral regions showing severe atrophy	Pathological subtype	Reference
1/M	34	6.3	Weakness in the left hand, dysarthria	Lower motor neuron signs	Temporal pole	BIBD	[19,26,31]
2/M	57	6	Obsessive behaviors	Behavioral abnormality	Frontal pole, temporal pole, temporal base	BIBD	[5,10,19,27,31]
3/F	56	12	Behavioral abnormality, memory impairment, altered eating habit	Behavioral abnormality	Frontal pole, temporal pole temporal base	BIBD	[5,10,19,28,31]
4/M	40	7	Disinhibition	Behavioral abnormality	Frontal base temporal base	BIBD	[19]
5/M	44	3.3	Overeating	Behavioral abnormality	Anterior portion of frontal convexity	BIBD	[32]
6/F	67	5.7	Dysarthria	Pseudobulbar palsy, nonfluent aphasia	Posterior portion of frontal convexity	NIFID	[19,29,31]
7/M	29	8	Disinhibition	Behavioral abnormality	Posterior portion of frontal convexity, temporal pole	NIFID	[19,33]
8/M	39	13	Apathy, behavioral abnormality	Behavioral abnormality	Temporal pole, temporal base	aFTLD-U	
9/F	30	15	Behavioral abnormality, memory impairment	Behavioral abnormality	Frontal convexity	Unclassifiable	[25,30]

Additional features: cases 1, 2, 4 and 6 were associated with parkinsonism. Case 6 was associated with lower motor neuron signs in the terminal stage.

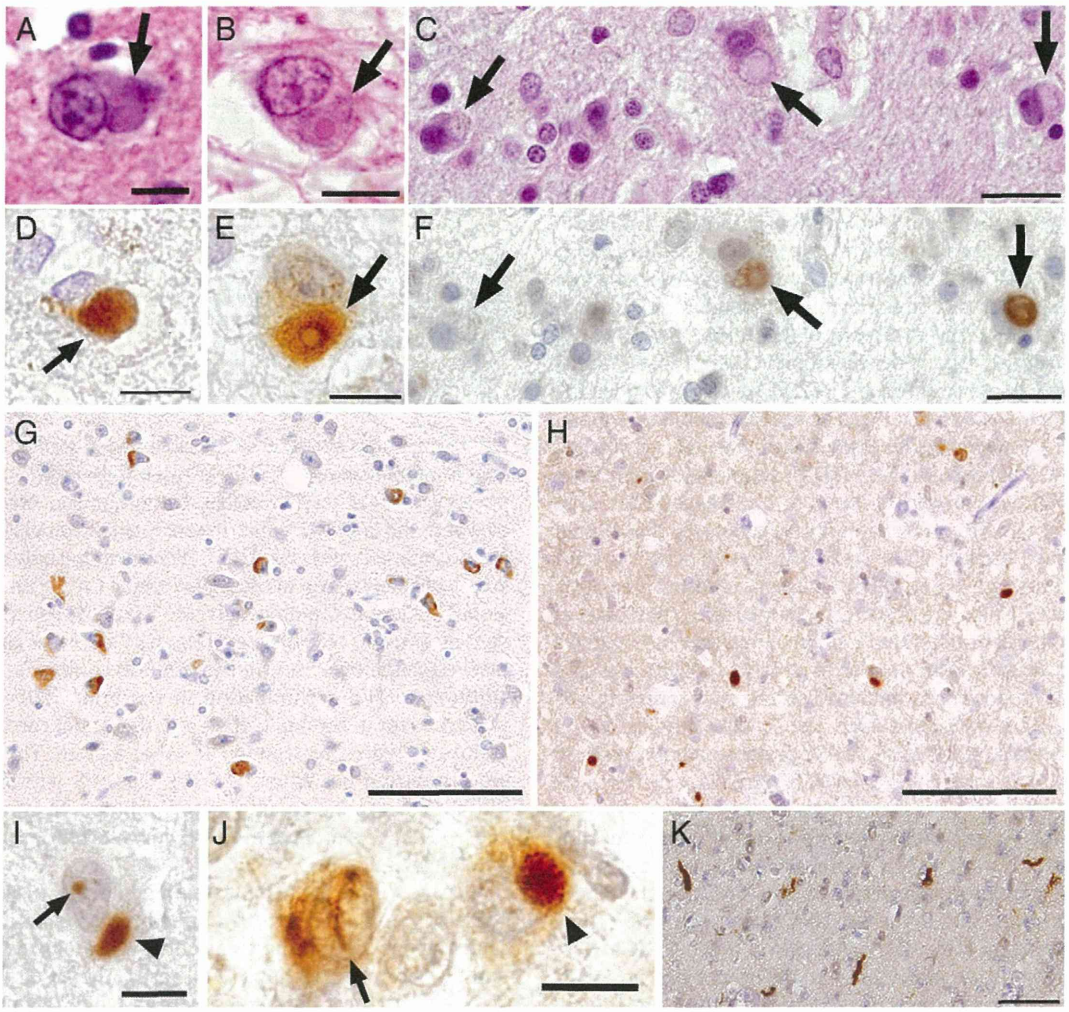

Fig. 1. A: hematoxylin and eosin (HE) staining of the frontal cortex of a BIBD case, case 5. The neuronal cytoplasmic inclusion (NCI) has a thin basophilic rim (arrow). B: HE staining of the hippocampus of an NIFID case, case 6. The NCI (arrow) in a pyramidal neuron contains a distinct eosinophilic core. C: HE staining of the frontal cortex of another NIFID case, case 7. The arrows indicate NCIs. The central compartments of NCIs were faintly stained and outlined by relatively intense staining. D: an α-internexin positive NCI in case 6. Panels E through K are immunostaining for FUS [86–213]. E: a FUS positive inclusion with a core (arrow) in the hippocampus of an NIFID case, case 6. The core is stained only weakly. F: the section shown in C was destained and restained immunohistochemically for FUS [86–213]. Immunoreactivity of the inclusions for FUS is variable (arrows). G: multiform – annular, crescent, tangle-like and oval – NCIs in the frontal cortex of a BIBD case, case 5. H: round NCIs in the frontal cortex of an a-FTLD-U case, case 8. I: a round neuronal intranuclear inclusion (NII) (arrow) and an NCI (arrowhead) in the hippocampus of an NIFID case, case 7. J: the hippocampus of an aFTLD-U case, case 8. The arrow and arrowhead indicate a vermiform NII and a NCI (arrowhead), respectively. K: FUS positive dystrophic neurites (DNs) in case 9. Scale bars are 10 μm in A, B, D, E, I and J; 20 μm in C and F; 50 μm in G and H; 50 μm in K.

the nuclei (Figs. 2A, B and 3A insert). When we raised the concentration of the antibody, both NCIs and the nuclei became positive (Fig. 3A). In some patients, however, only NCIs were labeled even at the highest possible concentration of the antibody, at which high background staining began to cloud the specific labeling. In type N, positive staining of the nuclei appeared first, and then NCIs became positive at higher concentrations of the antibody. Similarly to type I, only the nuclei were labeled in some patients, even at the highest possible concentration of the antibody. Figs. 2C, D and 3B illustrate nuclear labeling in the absence of NCIs staining at a low concentration of an antibody.

The staining patterns of each antibody in all cases are summarized in Table 3. In all cases, two antibodies to the middle portions of FUS, anti-FUS [52–400] and anti-FUS [86–213], showed the type I pattern. These two antibodies, particularly anti-FUS [86–213], were those most frequently used in the literature. While anti-FUS [250–300] did not work well in a number of cases, this antibody also showed the type I pattern when it worked. Antibodies to the carboxyl terminal portions, anti-FUS [400–450] and anti-FUS [500–526], on the other hand, showed the type N pattern in most, if not all, cases. The staining pattern of the two antibodies to the amino-terminal portion, anti-FUS [1–50] from different sources, varied among cases but was type I in both NIFID cases and type N in 4 of 5 BIBD cases.

4. Discussion

Whereas an accurate incidence of the disease cannot be determined by examination of an institutional brain collection, FTLD-FUS comprised approximately 14% of all FTLD in the present study. If one considers the selection bias for autopsies of clinically unusual FTLD cases, such frequencies may be fairly comparable with or only a little more than those reported in western countries [6,7,9,12]. A clear difference, however, does exist in the ratios of FTLD-FUS subtypes. In this FTLD-FUS archive, only one case had pathology consistent with aFTLD-U, which is the most common subtype of FTLD-FUS in western countries [5,13,14]. Again, a selection bias for autopsies of cases with movement disorders might be present and increase BIBD and NIFID relative to aFTLD-U. However, the difference may be too large to be

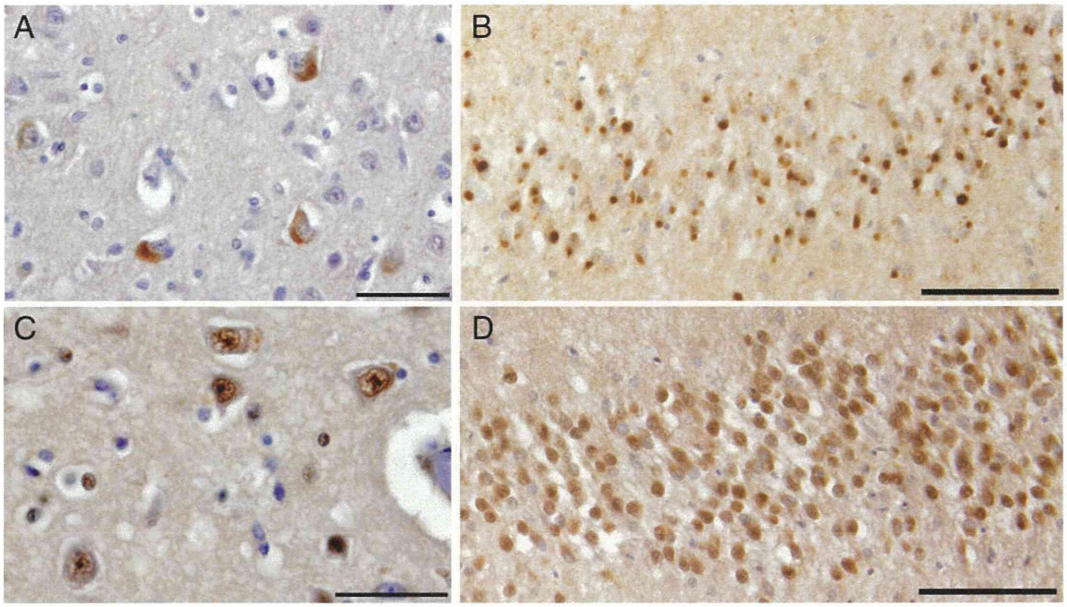

Fig. 2. A, C: High power photomicrographs of the frontal cortex, layer III, of a BIBD case. B, D: The granular cell layer of the hippocampal dentate gyrus of an NIFID case. The anti-FUS [52–400] antibody labels only NCIs but not the nuclei at a concentration of 13 μg/ml (A, B), showing the type I pattern. The anti-FUS [400–450] antibody hardly stains NCIs but well stains the nuclei at a concentration of 50 μg/ml (C, D), showing the type N pattern. Scale bars are 50 μm (A, C) and 100 μm (B, D).

explained by such a bias because nearly half of the cases in this archive lacked clinically evident movement disorders (Table 2). Furthermore, this aFTLD-U case did not seem to be typical in that NIIs occurred only occasionally, even in the dentate gyrus of the hippocampus. Such a feature rather suggests some pathological overlap with BIBD in this case. An ethnic difference present in sporadic diseases, i.e., a distinct subtype frequency, may suggest that some yet unidentified genetic background or environmental factors influence the pathophysiology of FTLD-FUS.

Comparison of FUS positive inclusions between BIBD and NIFID largely confirmed observations by Mackenzie et al. [5]. In one of the cases of NIFID, case 6, the NCIs bearing eosinophilic cores were α-internexin negative [19] but FUS positive. The cores themselves were negative or weakly positive for FUS, however. Even after extensive observation, we were not able to find NIIs in case 6. NIIs were present in case 7 but this case lacked NCIs with eosinophilic cores. While both cases with and without NCIs with eosinophilic cores have been classified into NIFID [11], it seems that there still remains a possibility that NIFID consists of heterogenous diseases [18]. At any event, the limited number of cases did not permit further analyses in the present study.

At present, the mechanisms by which α-internexin and neurofilament proteins are deposited in some NCIs in FTLD-FUS remain unclear. Neuronal intermediate filament proteins, such as α-internexin, are known to be accumulated in the neuronal cytoplasm in many degenerative diseases [16], as well as in a model of axonal transport disruption by brain injury [34,35]. In this study, we found α-internexin positive NCIs in two BIBD, cases 1 and 4, a finding consistent with a previous report [5]. In addition, we saw diffuse cytoplasmic accumulation of α-internexin in the brain regions with degenerative changes. It has to be noted that such intense cytoplasmic staining was often indistinguishable from labeling of NCIs. It seems that NIFID and other subtypes of FTLD-FUS can not always be distinguished with certainty by α-internexin immunohistochemistry.

In the present study, we have revealed that the nuclei and NCIs/DNs have different immunohistochemical profiles, depending on the portions of FUS that are recognized by the antibodies. Antibodies to the carboxyl terminal portion of FUS show a nuclei-dominant staining pattern, a finding which indicates that the carboxyl terminal portion of the FUS molecule is easier to be accessed in the nuclei than in NCIs/DNs. Antibodies to the middle portion of FUS, on the other hand, show a NCIs/DNs-dominant staining pattern, indicating that the middle portion can be more readily accessed in NCIs/DNs than in the nuclei. DNs in the atypical case, case 9, with DNs-dominant FUS accumulation in the cerebral cortex also showed a similar immunohistochemical profile to NCIs/DNs in other cases. A weakness of these findings is that they rely on the results obtained in formalin-fixed, paraffin-embedded tissue sections treated with heat for antigen retrieval. Sensitivity of FUS immunohistochemistry is known to be decreased by prolonged formalin fixation. All brains employed in the present study were formalin-fixed for long periods that varied from several weeks to months.

However, in well-controlled and lightly-fixed tissues that do not require antigen retrieval pretreatment, the immunohistochemical profiles of FUS also differ in normal brain between the nucleus and the dendrites/synapses [36]. The immunohistochemical profile of FUS in NCIs/DNs is close to that of cytoplasmic FUS in the dendrites/synapses. It may be noteworthy that cytoplasmic FUS is increased in pathological conditions [36], and that translocation of FUS from the nucleus to cytoplasm has been implicated in the pathogenesis of FUS proteinopathy [7,21,37]. The results of this study seem to be consistent with these recent observations. At present, whether such a difference is derived from a conformational change, or complex formation with other molecules, remains unknown. Though the low incidence of FUS proteinopathy causes difficulty in analyzing the biochemical natures of FUS abnormalities, further efforts have to be made to unveil the molecular basis for FUS accumulation in diseased conditions.

Supplementary data to this article can be found online at http://dx.doi.org/10.1016/j.jns.2013.08.035.

Acknowledgment

This work was supported in part by grants from Ministry of Health, Labor and Welfare (13800916), and Ministry of Education, Culture, Science (24500429, 221S003), Japan. The authors do not have any conflicts of interest or commercial relationships.

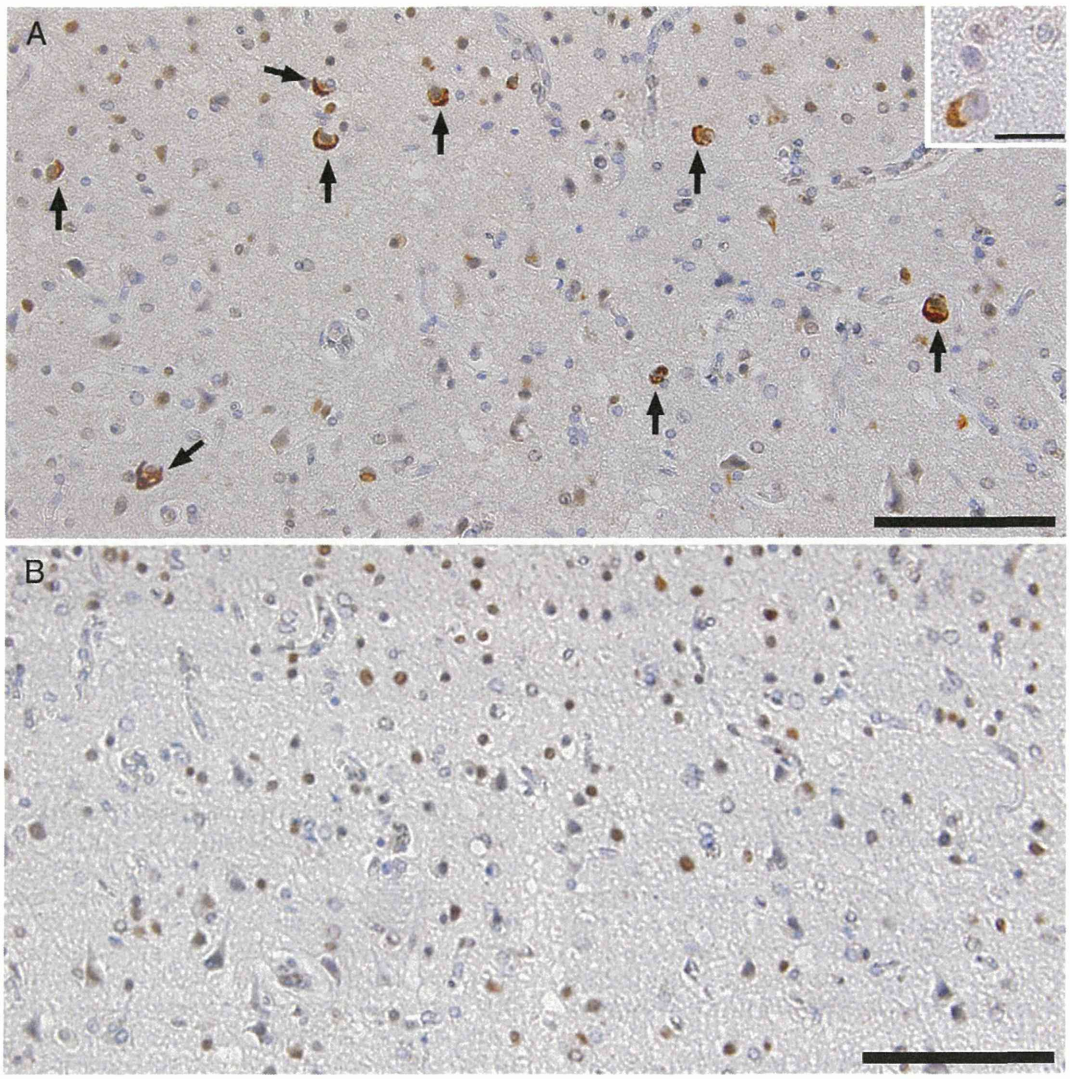

Fig. 3. Layers II and III of the frontal cortex of an NIFID case. A: Immunostaining with anti-FUS [86–213] at a concentration of 6.25 μg/ml. Both NCIs (arrows) and the nuclei are positive, but NCIs are more intensely stained than the nuclei. The insert shows a photomicrograph taken from a nearby section stained at a lower concentration (1.25 μg/ml) of the same antibody. Only the inclusion is positive and the nuclei are not labeled. Thus, this antibody shows the type I pattern in this case. B: Immunostaining with anti-FUS [500–526] at a concentration of 10 μg/ml. Only the nuclei are stained positively and NCIs remain unstained at this concentration of the antibody, showing the type N pattern. Scale bars are 100 μm (A, B) and 20 μm (*insert* in A).

References

[1] Kwiatkowski Jr TJ, Bosco DA, Leclerc AL, Tamrazian E, Vanderburg CR, Russ C, et al. Mutations in the FUS/TLS gene on chromosome 16 cause familial amyotrophic lateral sclerosis. Science 2009;323:1205–8.
[2] Vance C, Rogelj B, Hortobágyi T, De Vos KJ, Nishimura AL, Sreedharan J, et al. Mutations in FUS, an RNA processing protein, cause familial amyotrophic lateral sclerosis type 6. Science 2009;323:1208–11.
[3] Neumann M, Rademakers R, Roeber S, Baker M, Kretzschmar HA, Mackenzie IR. A new subtype of frontotemporal lobar degeneration with FUS pathology. Brain 2009;132:2922–31.
[4] Mackenzie IR, Neumann M, Bigio EH, Cairns NJ, Alafuzoff I, Kril J, et al. Nomenclature and nosology for neuropathologic subtypes of frontotemporal lobar degeneration: an update. Acta Neuropathol 2010;119:1–4.
[5] Mackenzie IR, Munoz DG, Kusaka H, Yokota O, Ishihara K, Roeber S, et al. Distinct pathological subtypes of FTLD-FUS. Acta Neuropathol 2011;121:207–18.
[6] Rohrer JD, Lashley T, Schott JM, Warren JE, Mead S, Isaacs AM, et al. Clinical and neuroanatomical signatures of tissue pathology in frontotemporal lobar degeneration. Brain 2011;134:2565–81.
[7] Halliday G, Bigio EH, Cairns NJ, Neumann M, Mackenzie IR, Mann DM. Mechanisms of disease in frontotemporal lobar degeneration: gain of function versus loss of function effects. Acta Neuropathol 2012;124:373–82.
[8] Armstrong RA, Gearing M, Bigio EH, Cruz-Sanchez FF, Duyckaerts C, Mackenzie IR, et al. The spectrum and severity of FUS-immunoreactive inclusions in the frontal and temporal lobes of ten cases of neuronal intermediate filament inclusion disease. Acta Neuropathol 2011;121:219–28.
[9] Mackenzie IR, Rademakers R, Neumann M. TDP-43 and FUS in amyotrophic lateral sclerosis and frontotemporal dementia. Lancet Neurol 2010;9:995–1007.
[10] Munoz DG, Neumann M, Kusaka H, Yokota O, Ishihara K, Terada S, et al. FUS pathology in basophilic inclusion body disease. Acta Neuropathol 2009;118:617–27.
[11] Neumann M, Roeber S, Kretzschmar HA, Rademakers R, Baker M, Mackenzie IR. Abundant FUS-immunoreactive pathology in neuronal intermediate filament inclusion disease. Acta Neuropathol 2009;118:605–16.
[12] Snowden JS, Hu Q, Rollinson S, Halliwell N, Robinson A, Davidson YS, et al. The most common type of FTLD-FUS (aFTLD-U) is associated with a distinct clinical form of frontotemporal dementia but is not related to mutations in the FUS gene. Acta Neuropathol 2011;122:99–110.
[13] Rohrer JD, Lashley T, Holton J, Revesz T, Urwin H, Isaacs AM, et al. The clinical and neuroanatomical phenotype of FUS associated frontotemporal lobar degeneration. J Neurol Neurosurg Psychiatry 2011;82:1405–7.
[14] Urwin H, Josephs KA, Rohrer JD, Mackenzie IR, Neumann M, Authier A, et al, FReJA Consortium. FUS pathology defines the majority of tau- and TDP-43-negative frontotemporal lobar degeneration. Acta Neuropathol 2010;120:33–41.
[15] Cairns NJ, Grossman M, Arnold SE, Burn DJ, Jaros E, Perry RH, et al. Clinical and neuropathologic variation in neuronal intermediate filament inclusion disease. Neurology 2004;63:1376–84.
[16] Cairns NJ, Uryu K, Bigio EH, Mackenzie IR, Mackenzie IR, Gearing M, et al. Alpha-internexin aggregates are abundant in neuronal intermediate filament inclusion disease (NIFID) but rare in other neurodegenerative diseases. Acta Neuropathol 2004;108:213–23.
[17] Josephs KA, Holton JL, Rossor MN, Braendgaard H, Ozawa T, Fox NC, et al. Neurofilament inclusion body disease: a new proteinopathy? Brain 2003;126:2291–303.

[18] Gelpi E, Llado A, Clarimon J, Rey MJ, Rivera RM, Ezquerra M, et al. Phenotypic variability within the inclusion body spectrum of basophilic inclusion body disease and neuronal intermediate filament inclusion disease in frontotemporal lobar degenerations with FUS-positive inclusions. J Neuropathol Exp Neurol 2012;71:795–805.
[19] Yokota O, Tsuchiya K, Terada S, Ishizu H, Uchikado H, Ikeda M, et al. Basophilic inclusion body disease and neuronal intermediate filament inclusion disease: a comparative clinicopathological study. Acta Neuropathol 2008;115:561–75.
[20] Neumann M, Bentmann E, Dormann D, Jawaid A, DeJesus-Hernandez M, Ansorge O, et al. FET proteins TAF15 and EWS are selective markers that distinguish FTLD with FUS pathology from amyotrophic lateral sclerosis with FUS mutations. Brain 2011;134:2595–609.
[21] Neumann M, Valori CF, Ansorge O, Kretzschmar HA, Munoz DG, Kusaka H, et al. Transportin 1 accumulates specifically with FET proteins but no other transportin cargos in FTLD-FUS and is absent in FUS inclusions in ALS with FUS mutations. Acta Neuropathol 2012;124:705–16.
[22] Ikeda M, Ishikawa T, Tanabe H. Epidemiology of frontotemporal lobar degeneration. Dement Geriatr Cogn Disord 2004;17:265–8.
[23] Ikeda K. Neuropathological discrepancy between Japanese Pick's disease without Pick bodies and frontal lobe degeneration type of frontotemporal dementia proposed by Lund and Manchester Group. Neuropathology 2000;20:76–82.
[24] Ogaki K, Li Y, Takanashi M, Ishikawa K, Kobayashi T, Nonaka T, et al. Analyses of the MAPT, PGRN, and C9orf72 mutations in Japanese patients with FTLD, PSP, and CBS. Parkinsonism Relat Disord 2013;19:15–20.
[25] Kobayashi Z, Arai T, Yokota O, Tsuchiya K, Hosokawa M, Oshima K, et al. Atypical FTLD-FUS associated with ALS-TDP: a case report. Neuropathology 2013;33:83–8.
[26] Dobutsu M, Hanyu S, Yosida M, Oyanagi S. Immunohistochemical and ultrastructural investigation of argyrophilic neuronal cytoplasmic inclusions in a patient with ALS-like symptoms, dementia, cerebellar ataxia and extrapyramidal symptoms (in Japanese with English abstract). Neuropathology 1993;13:31–8.
[27] Ishino H, Yokoyama S, Nakashima Y, Otsuki S, Morisada A. Atrophy of basal ganglia in Pick's disease (in Japanese with English abstract). Kyushu Neuropsychiatry 1971;17:67–73.
[28] Kuyama K, Kuroda S, Morioka E, Oda T. Pick's disease with argyrophilic inclusions in the basal ganglia and brainstem. in Japanese with English abstract Neuropathology 1987;8:35–44.
[29] Sakajiri K, Bandou M, Yamanouchi H, Ishii K, Fukusako Y. Slowly progressive dysarthria and impaired language function — a case report, 32. Rinsho Shinkeigaku; 1992. p. 1107–11 [in Japanese].
[30] Tsuchiya K, Ikeda K, Haga C, Kobayashi T, Morimatsu Y, Nakano I, et al. Atypical amyotrophic lateral sclerosis with dementia mimicking frontal Pick's disease: a report of an autopsy case with a clinical course of 15 years, 101. Acta Neuropathol; 2001. p. 625–30.
[31] Tsuchiya K, Ishizu H, Nakano I, Fukui T, Kuroiwa T, Haga C, et al. Distribution of basal ganglia lesions in generalized variant of Pick's disease: a clinicopathological study of four autopsy cases. Acta Neuropathol 2001;102:441–8.
[32] Yoshida T, Matsushita M, Nagao Y, Takahashi Y. A case of the frontal type of Pick's disease — with special reference to the frontal lobe syndrome and "running-away" behavior. in Japanese with English abstract Seishinshinkeigaku Zasshi 1981;83:129–46.
[33] Yamasue H, Tsuchiya K, Kuroki N, Honada M, Niizato K, Anno M, et al. A clinical case of sporadic frontal Pick's disease with onset at 29 years old of age. in Japanese with English abstract Seishin Igaku 2000;42:1271–7.
[34] Smith DH, Chen XH, Nonaka M, Trojanowski JQ, Lee VM, Saatman KE, et al. Accumulation of amyloid beta and tau and the formation of neurofilament inclusions following diffuse brain injury in the pig. J Neuropathol Exp Neurol 1999;58:982–92.
[35] Hamberger A, Huang YL, Zhu H, Bao F, Ding M, Blennow K, et al. Redistribution of neurofilaments and accumulation of beta-amyloid protein after brain injury by rotational acceleration of the head. J Neurotrauma 2003;20:169–78.
[36] Aoki N, Higashi S, Kawakami I, Kobayashi Z, Hosokawa M, Katsuse O, et al. Localization of fused in sarcoma (FUS) protein to the post-synaptic density in the brain. Acta Neuropathol 2012;124:383–94.
[37] Brelstaff J, Lashley T, Holton JL, Lees AJ, Rossor MN, Bandopadhyay R, et al. Transportin1: a marker of FTLD-FUS. Acta Neuropathol 2011;22:591–600.

Journal of the Neurological Sciences 335 (2013) 224–227

Contents lists available at ScienceDirect

Journal of the Neurological Sciences

journal homepage: www.elsevier.com/locate/jns

Short communication

Thalamic hypoperfusion in early stage of progressive supranuclear palsy (Richardson's syndrome): Report of an autopsy-confirmed case

Zen Kobayashi [a,*], Miho Akaza [a], Shoichiro Ishihara [b], Hiroyuki Tomimitsu [a], Yukinori Inadome [c], Tetsuaki Arai [d], Haruhiko Akiyama [e], Shuzo Shintani [a]

[a] Department of Neurology, JA Toride Medical Center, Ibaraki, Japan
[b] Department of Neurology and Neurological Science, Tokyo Medical and Dental University, Tokyo, Japan
[c] Department of Pathology, JA Toride Medical Center, Ibaraki, Japan
[d] Department of Psychiatry, Graduate School of Comprehensive Human Sciences, University of Tsukuba, Ibaraki, Japan
[e] Tokyo Metropolitan Institute of Medical Science, Tokyo, Japan

ARTICLE INFO

Article history:
Received 21 June 2013
Received in revised form 28 August 2013
Accepted 4 September 2013
Available online 13 September 2013

Keywords:
Progressive supranuclear palsy
Richardson's syndrome
Midbrain
Thalamus
MRI
SPECT

ABSTRACT

Progressive supranuclear palsy-Richardson's syndrome (PSP-RS) is a neurodegenerative disease characterized by postural instability and vertical gaze palsy, but the clinical diagnosis of PSP-RS is often difficult in the early stage of the disease. A 64-year-old male experienced frequent falls, followed by dysarthria and dysphagia. Neurological examination at age 64 demonstrated vertical gaze palsy, dysarthria, dysphagia, and retropulsion. At that time, while brain MRI demonstrated no apparent abnormalities, SPECT showed the reduction of the cerebral blood flow in the thalamus as well as the medial frontal lobe cortices. The patient was diagnosed with probable PSP-RS, and died at age 70. On postmortem examination, there were abundant tuft-shaped astrocytes, neurofibrillary tangles, coiled bodies, and argyrophilic threads in the brain, establishing the diagnosis of PSP-RS. Our definite PSP-RS case suggests that thalamic hypoperfusion may provide helpful evidence to support a diagnosis of PSP-RS in the early stage of the disease.

1. Introduction

Progressive supranuclear palsy (PSP) was originally described as a neurodegenerative disease showing postural instability, vertical gaze palsy, pseudobulbar palsy, nuchal dystonia, and cognitive impairment [1]. Currently, this original disease is sometimes called as Richardson's syndrome (RS) or PSP-RS to distinguish from atypical PSP known as PSP-parkinsonism (PSP-P) [2]. In PSP-RS, death usually occurs within 5–7 years [3–6]. The clinical diagnosis of probable PSP-RS requires the presence of a gradually progressive disorder with onset at age 40 or later, vertical supranuclear gaze palsy, prominent postural instability, falls in the first year of onset, and no evidence of other diseases that could explain these features [4]. Although midbrain atrophy has been reported as a characteristic MRI finding of the patients with autopsy-confirmed PSP-RS [7,8], this abnormality is absent or subtle in the early stage of the disease. The early clinical diagnosis of PSP-RS is therefore often difficult, but is important for deciding on the treatment and management of patients. Recent studies using functional brain images have shown the involvement of the frontal lobe cortex and thalamus in patients with probable PSP-RS [9–11]. In addition, some studies demonstrated that thalamic involvement was a finding that distinguishes PSP-RS from PSP-P, Parkinson's disease, or multiple system atrophy [9,11,12].

While definite PSP-RS requires histopathologic evidence of PSP [4], the brain pathology of some cases showing clinical features of PSP-RS is not PSP pathology but corticobasal degeneration, frontotemporal dementia associated with chromosome 17, multiple system atrophy, dementia with Lewy bodies, or sporadic Creutzfeldt–Jakob disease (sCJD) [13–17]. One study showed that 43 out of 180 clinical PSP cases had brain pathology other than that of PSP [13]. At present, it remains unclear whether thalamic involvement on functional brain images is demonstrated from the early stage of definite PSP-RS and can be used as an early diagnostic marker. Here, we report a case of definite PSP-RS in which thalamic hypoperfusion was demonstrated in the early stage of the disease.

2. Case report

A 64-year-old male experienced frequent falls, followed by dysarthria and dysphagia, and consulted our hospital. The past medical history included chronic hepatitis C. There was no consanguinity or family history of neurological diseases. Neurological examination at age 64 demonstrated vertical gaze palsy, dysarthria, dysphagia, and retropulsion. There was no apparent dementia, muscle rigidity, tremor, akinesia,

* Corresponding author at: Department of Neurology, JA Toride Medical Center, 2-1-1 Hongo, Toride, Ibaraki 302-0022, Japan.
E-mail address: zen@bg7.so-net.ne.jp (Z. Kobayashi).

0022-510X/$ – see front matter © 2013 Elsevier B.V. All rights reserved.
http://dx.doi.org/10.1016/j.jns.2013.09.005

motor weakness, or autonomic failure. On T1-weighted images of brain MRI at age 64, midbrain atrophy was not apparent (Fig. 1A, B), but the superior surface of the midbrain showed a flat aspect (Fig. 1A), suggesting the presence of slight atrophy of the rostral midbrain tegmentum [18]. There was no apparent enlargement of the third ventricle (Fig. 1C, D) or frontal lobe atrophy. Fluid attenuated inversion recovery (FLAIR) images demonstrated no abnormal signal intensities in the brain including the thalamus. However, brain SPECT conducted on the same day showed the reduction of the cerebral blood flow (CBF) not only in the medial frontal lobe cortices but also the bilateral thalamus with a left predominance (Fig. 2A). Regional CBF was compared with the age-matched database of eZIS (version 3. FUJIFILM RI Pharma) [19,20]. Images of eZIS demonstrated regions showing a Z-score of 2 or more in the medial frontal lobe cortices and thalamus (Fig. 2B). At age 65, muscle rigidity became evident in the neck and four limbs, and hyperreflexia was also demonstrated. The patient was considered to have probable PSP-RS. Subsequently, parkinsonism gradually progressed and responded poorly to carbidopa/levodopa.

From age 68, the patient showed repeated aspiration pneumonia and was admitted to our hospital 4 times within 16 months. Cognitive impairment and akinesia became apparent. At age 68, percutaneous endoscopic gastrostomy was performed for dysphagia. On brain MRI at age 68, there was evident atrophy of the midbrain tegmentum (Fig. 1E, F), slight enlargement of the third ventricle (Fig. 1G, H), and frontal lobe atrophy. At age 69, a diagnosis of hepatocellular carcinoma was made. The patient died of rupture of hepatocellular carcinoma at age 70. The total clinical course was about 6 years.

3. Autopsy findings

The brain weight was 1269 g before fixation. The left half of the brain was processed for neuropathologic studies. Brain and spinal cord tissue samples were fixed postmortem with 10% formalin. External examination demonstrated mild atrophy of the dorsolateral and medial frontal lobe, and anterior temporal lobe. On the sections, enlargement of the lateral ventricle was moderate in the anterior horn, and was mild in the inferior horn. The volume of the frontal lobe white matter was reduced. The caudate head, putamen, globus pallidus, and thalamus were all slightly atrophic. The substantia nigra was atrophic and depigmented. Depigmentation was also noted in the locus ceruleus, but was mild when compared to that of the substantia nigra.

After embedding the tissue samples in paraffin, 10-micrometer-thick (multiple 10-μm-thick) sections were prepared from the cerebrum, midbrain, pons, medulla oblongata, cerebellum, and spinal cord. The sections were stained with hematoxylin–eosin (HE) and Klüver–Barrera (KB) and by the Gallyas–Braak method, and were examined immunohistochemically by the immunoperoxidase method using 3,3′-diaminobenzidine tetrahydrochloride and hematoxylin as the chromogen and counterstain, respectively. We used anti-tau antibodies (AT8, mouse, monoclonal, Innogenetics, Gent, Belgium 1:2000) for immunohistochemistry.

Microscopically, neuron loss was severe in the substantia nigra and subthalamic nucleus, moderate in the locus ceruleus and cerebellar dentate nucleus, and mild in the frontal lobe cortex, caudate nucleus, putamen, globus pallidus, and thalamus. There were no spongiform changes in the cerebral cortex suggesting sCJD. Grumose degeneration was noted in the remaining neurons of the cerebellar dentate nucleus. The pedunculopontine nucleus could not be evaluated. Gallyas staining and tau immunohistochemistry demonstrated tuft-shaped astrocytes (Fig. 3A) in the dorsolateral frontal lobe, basal ganglia, and thalamus, establishing a diagnosis of definite PSP-RS. In addition, there were abundant neurofibrillary tangles, coiled bodies (Fig. 3B), and argyrophilic threads in the dorsolateral frontal lobe, caudate nucleus, putamen, globus pallidus, thalamus, subthalamic nucleus, mammillary body, substantia nigra, locus ceruleus, pontine nucleus, cerebellar dentate nucleus, and inferior olivary nucleus. A few neurofibrillary tangles were also noted in the transentorhinal and entorhinal cortices, and hippocampal CA1. The distribution of the brain lesions in our case was mostly consistent with that of typical PSP-RS cases [21].

4. Discussion

While midbrain atrophy or enlargement of the third ventricle was not apparent on brain MRI at first in our patient, SPECT had already shown thalamic involvement. These findings suggest that thalamic hypoperfusion on SPECT may provide evidence to support a diagnosis

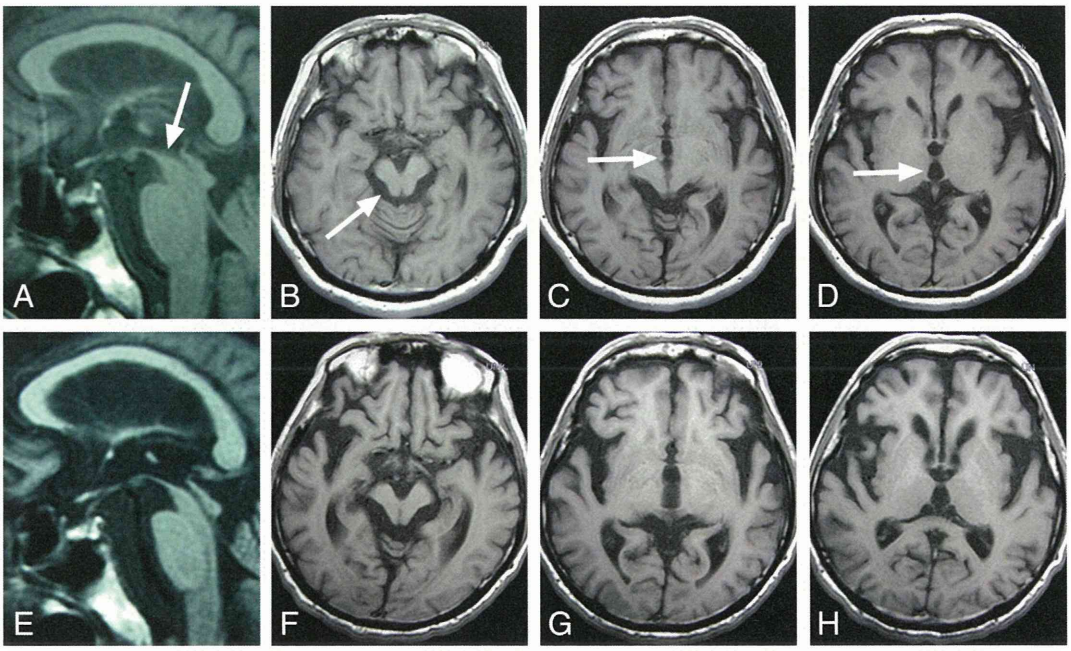

Fig. 1. On a midline sagittal T1-weighted image of brain MRI at age 64 (A), the superior surface of the midbrain showed a flat aspect (arrow), suggesting the presence of slight atrophy of the rostral midbrain tegmentum. On axial T1-weighted images at age 64 (B–D), there was no apparent atrophy of the midbrain tegmentum (B, arrow) or enlargement of the third ventricle (C, D, arrow). On midline sagittal (E) and axial (F–H) T1-weighted images at age 68, there was evident atrophy of the midbrain tegmentum (E, F) and slight enlargement of the third ventricle (G, H).

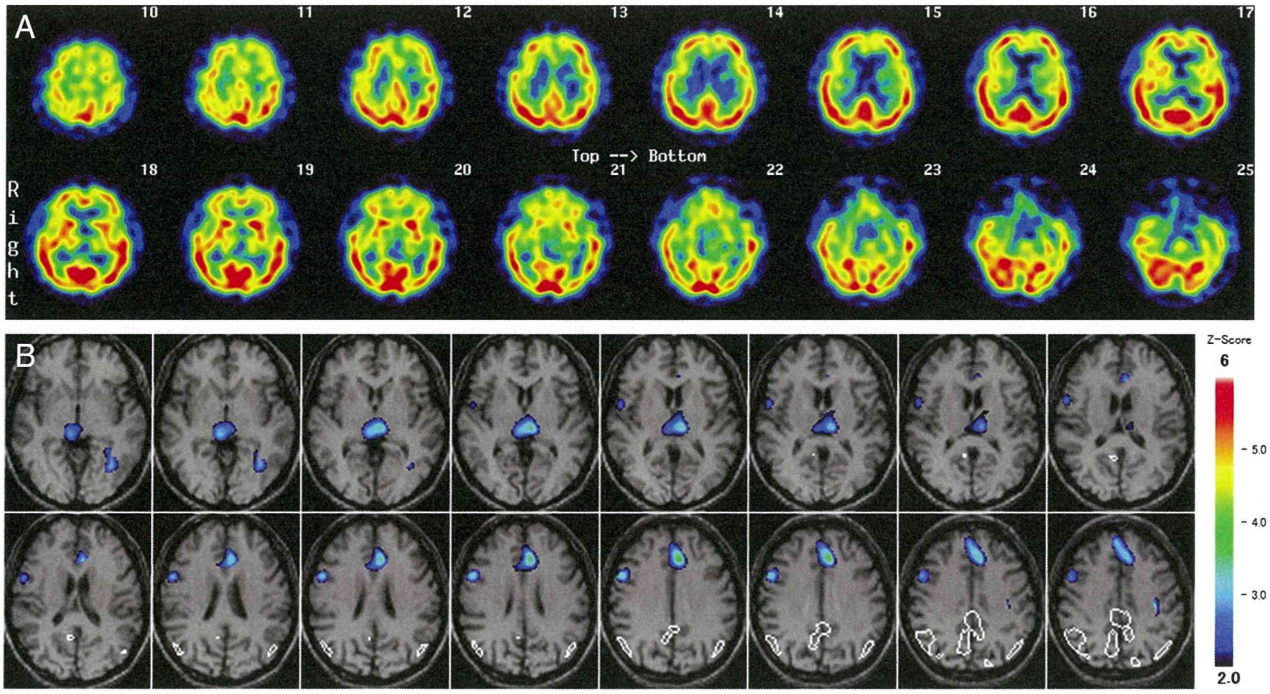

Fig. 2. Brain SPECT showed hypoperfusion in the bilateral thalamus with a left predominance as well as the medial frontal lobe cortices (A). Images of eZIS demonstrated regions showing a Z-score of 2 or more in the medial frontal lobe cortices and thalamus (B).

of PSP-RS in the early stage of the disease. In this patient, images of eZIS were useful to clearly demonstrate the brain regions showing hypoperfusion.

Recent studies using functional brain images have shown the involvement of the frontal lobe cortex and thalamus in patients with probable PSP-RS [9–11]. Because imbalance and falls as initial manifestations of most cases of PSP-RS are closely associated with thalamic dysfunction [22], thalamus may be involved from the early stage of PSP-RS. Intriguingly, thalamic involvement in patients with PSP-RS is considered to be a consequence of disrupted cholinergic fibers ascending from brainstem nuclei such as the pedunculopontine nuclei to thalamus rather than the impairment of cholinoceptive neurons in the thalamus [23]. This pathomechanism may explain the fact that thalamic degeneration is not necessarily severe in brains of autopsied patients with PSP-RS.

In neurodegenerative diseases, thalamic involvement on functional brain images has been reported not only in PSP-RS but also in the thalamic form of the MM2 subtype of sCJD [15], although the latter is extremely rare when compared to the former. Importantly, a proportion of patients with this type of sCJD present with clinical features of PSP-RS [15,16]. Because characteristic EEG and MRI abnormalities are almost absent in patients with this type of sCJD [15,16], a rapidly progressive course of PSP-RS may need the suspicion of an underlying sCJD pathology regardless of the absence of supportive findings on EEG or MRI [16].

So far, functional brain image findings have hardly been reported in patients with definite PSP-RS. While the study by Kimura et al. included one patient with definite PSP-RS, details of the clinical course of this patient are not described [11]. Thus, this is the first report of a case of definite PSP-RS in which thalamic involvement was demonstrated in the early stage of the disease. In the future, a large number of patients with PSP-RS should be studied employing functional brain images and autopsy to clarify whether thalamic involvement is a constant finding in the early stage of definite PSP-RS.

Conflict of interest statement

The authors have no conflicts of interest.

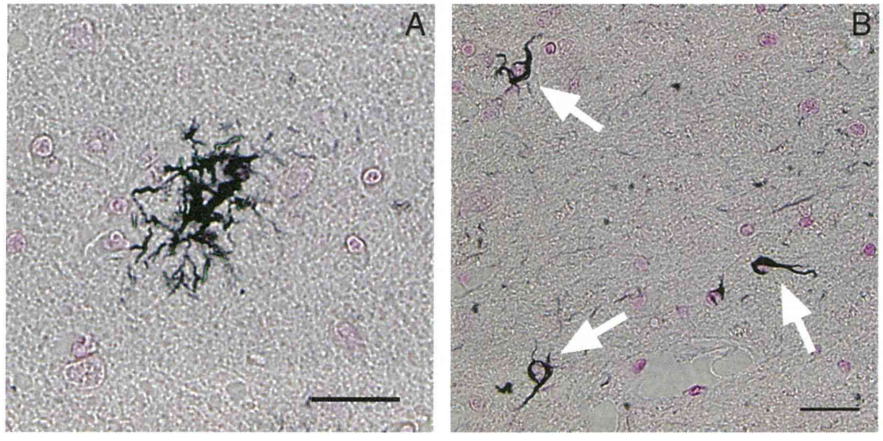

Fig. 3. Gallyas staining demonstrated a tuft-shaped astrocyte (A) and coiled bodies (B, arrows) in the frontal lobe cortices. Scale bars = 20 μm.

Acknowledgment

The authors thank Dr. Saneyuki Mizutani for clinical evaluation of the patient, Drs. Koji Unoura, Yoshiyuki Numasawa, and Ito Kawakami for the helpful comments.

References

[1] Steele JC, Richardson JC, Olszewski J. Progressive supranuclear palsy. A heterogenous degeneration involving the brain stem, basal ganglia and cerebellum with vertical gaze and pseudobulbar palsy, nuchal dystonia and dementia. Arch Neurol 1964;10:333–59.
[2] Williams DR, de Silva R, Paviour DC, Pittman A, Watt HC, Kilford L, et al. Characteristics of two distinct clinical phenotypes in pathologically proven progressive supranuclear palsy: Richardson's syndrome and PSP-parkinsonism. Brain 2005;128:1247–58.
[3] Nath U, Ben-Shlomo Y, Thomson RG, Lees AJ, Burn DJ. Clinical features and natural history of progressive supranuclear palsy: a clinical cohort study. Neurology 2003;60:910–6.
[4] Litvan I, Agid Y, Calne D, Campbell G, Dubois B, Duvoisin RC, et al. Clinical research criteria for the diagnosis of progressive supranuclear palsy (Steele–Richardson–Olszewski syndrome): report of the NINDS-SPSP international workshop. Neurology 1996;47:1–9.
[5] Litvan I, Mangone CA, McKee A, Verny M, Parsa A, Jellinger K, et al. Natural history of progressive supranuclear palsy (Steele–Richardson–Olszewski syndrome) and clinical predictors of survival: a clinicopathological study. J Neurol Neurosurg Psychiatry 1996;60:615–20.
[6] Papapetropoulos S, Singer C, McCorquodale D, Gonzalez J, Mash DC. Cause, seasonality of death and co-morbidities in progressive supranuclear palsy (PSP). Parkinsonism Relat Disord 2005;11:459–63.
[7] Slowinski J, Imamura A, Uitti RJ, Pooley RA, Strongosky AJ, Dickson DW, et al. MR imaging of brainstem atrophy in progressive supranuclear palsy. J Neurol 2008;255:37–44.
[8] Massey LA, Micallef C, Paviour DC, O'Sullivan SS, Ling H, Williams DR, et al. Conventional magnetic resonance imaging in confirmed progressive supranuclear palsy and multiple system atrophy. Mov Disord 2012;27:1754–62.
[9] Srulijes K, Reimold M, Liscic RM, Bauer S, Dietzel E, Liepelt-Scarfone I, et al. Fluorodeoxyglucose positron emission tomography in Richardson's syndrome and progressive supranuclear palsy-parkinsonism. Mov Disord 2012;27:151–5.
[10] Mazère J, Meissner WG, Mayo W, Sibon I, Lamare F, Guilloteau D, et al. Progressive supranuclear palsy: in vivo SPECT imaging of presynaptic vesicular acetylcholine transporter with [123I]-iodobenzovesamicol. Radiology 2012;265:537–43.
[11] Kimura N, Hanaki S, Masuda T, Hanaoka T, Hazama Y, Okazaki T, et al. Brain perfusion differences in parkinsonian disorders. Mov Disord 2011;26:2530–7.
[12] Agosta F, Pievani M, Svetel M, Ječmenica Lukić M, Copetti M, Tomić A, et al. Diffusion tensor MRI contributes to differentiate Richardson's syndrome from PSP-parkinsonism. Neurobiol Aging 2012;33:2817–26.
[13] Josephs KA, Dickson DW. Diagnostic accuracy of progressive supranuclear palsy in the Society for Progressive Supranuclear Palsy brain bank. Mov Disord 2003;18:1018–26.
[14] Osaki Y, Ben-Shlomo Y, Lees AJ, Daniel SE, Colosimo C, Wenning G, et al. Accuracy of clinical diagnosis of progressive supranuclear palsy. Mov Disord 2004;19:181–9.
[15] Hamaguchi T, Kitamoto T, Sato T, Mizusawa H, Nakamura Y, Noguchi M, et al. Clinical diagnosis of MM2-type sporadic Creutzfeldt–Jakob disease. Neurology 2005;64:643–8.
[16] Petrovic IN, Martin-Bastida A, Massey L, Ling H, O'Sullivan SS, Williams DR, et al. MM2 subtype of sporadic Creutzfeldt–Jakob disease may underlie the clinical presentation of progressive supranuclear palsy. J Neurol 2013;260:1031–6.
[17] Williams DR, Lees AJ. Progressive supranuclear palsy: clinicopathological concepts and diagnostic challenges. Lancet Neurol 2009;8:270–9.
[18] Righini A, Antonini A, De Notaris R, Bianchini E, Meucci N, Sacilotto G, et al. MR imaging of the superior profile of the midbrain: differential diagnosis between progressive supranuclear palsy and Parkinson disease. AJNR Am J Neuroradiol 2004;25:927–32.
[19] Kanetaka H, Matsuda H, Asada T, Ohnishi T, Yamashita F, Imabayashi E, et al. Effects of partial volume correction on discrimination between very early Alzheimer's dementia and controls using brain perfusion SPECT. Eur J Nucl Med Mol Imaging 2004;31:975–80.
[20] Matsuda H, Mizumura S, Nagao T, Ota T, Iizuka T, Nemoto K, et al. Automated discrimination between very early Alzheimer disease and controls using an easy Z-score imaging system for multicenter brain perfusion single-photon emission tomography. AJNR Am J Neuroradiol 2007;28:731–6.
[21] Hauw JJ, Daniel SE, Dickson D, Horoupian DS, Jellinger K, Lantos PL, et al. Preliminary NINDS neuropathologic criteria for Steele–Richardson–Olszewski syndrome (progressive supranuclear palsy). Neurology 1994;44:2015–9.
[22] Zwergal A, la Fougère C, Lorenzl S, Rominger A, Xiong G, Deutschenbaur L, et al. Postural imbalance and falls in PSP correlate with functional pathology of the thalamus. Neurology 2011;77:101–9.
[23] Hirano S, Shinotoh H, Shimada H, Aotsuka A, Tanaka N, Ota T, et al. Cholinergic imaging in corticobasal syndrome, progressive supranuclear palsy and frontotemporal dementia. Brain 2010;133:2058–68.

Liu et al. Acta Neuropathologica Communications 2013, 1:49
http://www.actaneurocomms.org/content/1/1/49

ACTA NEUROPATHOLOGICA COMMUNICATIONS

RESEARCH Open Access

Reducing TDP-43 aggregation does not prevent its cytotoxicity

Rui Liu[1], Guang Yang[1], Takashi Nonaka[2], Tetsuaki Arai[3], William Jia[1] and Max S Cynader[1*]

Abstract

Background: TAR DNA-binding protein 43 (TDP-43) is a protein that is involved in the pathology of Amyotrophic Lateral Sclerosis (ALS) and Frontotemporal Lobar Degeneration (FTLD). In patients with these neurodegenerative diseases, TDP-43 does not remain in its normal nuclear location, but instead forms insoluble aggregates in both the nucleus and cytoplasm of affected neurons.

Results: We used high density peptide array analysis to identify regions in TDP-43 that are bound by TDP-43 itself and designed candidate peptides that might be able to reduce TDP-43 aggregation. We found that two of the synthetic peptides identified with this approach could effectively inhibit the formation of TDP-43 protein aggregates in a concentration-dependent manner in HeLa cells in which a mutated human TDP-43 gene was overexpressed. However, despite reducing aggregation, these peptides did not reduce or prevent cell death. Similar results were observed in HeLa cells treated with arsenite. Again we found reduced aggregation, in this case of wild type TDP-43, but no difference in cell death.

Conclusions: Our results suggest that TDP-43 aggregation is associated with the cell death process rather than being a direct cause.

Keywords: TDP-43, Aggregation, Peptides, Cell death

Background

Recent evidence links TDP-43 pathology to at least two forms of neurodegeneration that had heretofore been thought to be quite separate. FTLD is the second most common type of early-onset neurodegenerative dementia after Alzheimer's disease, and ALS is the most common adult-onset progressive motor neuron disease (MND). The TAR DNA binding protein 43 (TDP-43) has been found to be the major protein constituent of the intracellular aggregated inclusions in both FTLD with ubiquitin-positive inclusions (FTLD-U) and ALS [1,2].

TDP-43 is a 414 amino acid protein encoded by the TARDBP gene on chromosome 1. It was originally identified as a transcriptional repressor of the human immunodeficiency virus type 1 (HIV-1) gene [3,4] and the mammalian gene SP-10 [5]. TDP-43 normally is found in the nucleus where it regulates RNA splicing, mRNA stability and microRNA processing [6-9], but TDP-43 in pathological inclusions is generally hyperphosphorylated, ubiquitinated [10], and cleaved to 35 and 25 kDa species [11]. The pathological aggregates are frequently found in the cytoplasm rather than at TDP-43's normal nuclear location [1,2,12].

The mechanism through which TDP-43 is involved in neuronal death and degeneration remains unclear. One of the best characterized pathological features of TDP-43 proteinopathies is the cytoplasmic inclusions of TDP-43 aggregates. As with other protein misfolding diseases, TDP-43 mediated toxicity may result from a toxic gain of function associated with its aggregation. Johnson and colleagues have established a yeast model involving over-expressed full-length human TDP-43 or various TDP-43 truncation products [13]. They found that expressing a truncated form of TDP-43 containing both the C-terminal and RRM2 promoted aggregation. Only the aggregated form of TDP-43 induced toxicity to yeast cells. This suggested that TDP-43 misfolding and aggregation might be an important cause of cell death in neurodegenerative diseases. Another group supported this conclusion in human cell models [14]. The 25 kDa

* Correspondence: cynader@brain.ubc.ca
[1]Brain Research Center, University of British Columbia, 2211 Wesbrook Mall, Vancouver, BC V6T2B5, Canada
Full list of author information is available at the end of the article